Journal of Magnetic Resonance **141,** 104–120 (1999)
Article ID jmre.1999.1895, available online at http://www.idealibrary.com on IDEAL®

Toward an *in Vivo* Neurochemical Profile: Quantification of 18 Metabolites in Short-Echo-Time ^{1}H NMR Spectra of the Rat Brain

Josef Pfeuffer,* Ivan Tkáč,* Stephen W. Provencher,† and Rolf Gruetter*

*Department of Radiology, University of Minnesota Medical School, Center for Magnetic Resonance Research, 2021 Sixth Street SE, Minneapolis, Minnesota 55455; and †Max Planck Institute for Biophysical Chemistry, Postfach 2841, 37070 Göttingen, Federal Republic of Germany

Received March 1, 1999; revised July 29, 1999

Localized *in vivo* ^{1}H NMR spectroscopy was performed with 2-ms echo time in the rat brain at 9.4 T. Frequency domain analysis with LCModel showed that the *in vivo* spectra can be explained by 18 metabolite model solution spectra and a highly structured background, which was attributed to resonances with fivefold shorter *in vivo* T_1 than metabolites. The high spectral resolution (full width at half maximum approximately 0.025 ppm) and sensitivity (signal-to-noise ratio approximately 45 from a 63-μL volume, 512 scans) was used for the simultaneous measurement of the concentrations of metabolites previously difficult to quantify in ^{1}H spectra. The strongly represented signals of *N*-acetylaspartate, glutamate, taurine, *myo*-inositol, creatine, phosphocreatine, glutamine, and lactate were quantified with Cramér–Rao lower bounds below 4%. Choline groups, phosphorylethanolamine, glucose, glutathione, γ-aminobutyric acid, *N*-acetylaspartylglutamate, and alanine were below 13%, whereas aspartate and *scyllo*-inositol were below 22%. Intra-assay variation was assessed from a time series of 3-min spectra, and the coefficient of variation was similar to the calculated Cramér–Rao lower bounds. Interassay variation was determined from 31 pooled spectra, and the coefficient of variation for total creatine was 7%. Tissue concentrations were found to be in very good agreement with neurochemical data from the literature. © 1999 Academic Press

Key Words: in vivo **^{1}H NMR spectroscopy; short echo time; rat brain; quantification; LCModel; macromolecules.**

INTRODUCTION

The usefulness of localized *in vivo* ^{1}H NMR spectroscopy at long and short echo times has been demonstrated in many studies of the brain and its disorders, e.g., in hepatic encephalopathy, Alzheimer's, Huntington's, and Parkinson's diseases, acute traumatic brain injury, and dementia (*1*, *2*). When using long echo times (>100 ms), spectra are simplified and the dominant singlet peaks of the methyl groups are readily observable. Most ^{1}H NMR investigations *in vivo* have focused on detecting changes of the methyl signals of, *N*-acetylaspartate (NAA),[1] total creatine (Cr + PCr), choline (Cho), and lactate (Lac) (*3–5*). Short-echo-time *in vivo* ^{1}H NMR spectra contain more information, i.e., increased signal contributions of coupled spin systems such as glutamate (Glu), glutamine (Gln), *myo*-inositol (Ins), glucose (Glc), and taurine (Tau). The ensuing spectral overlap requires sophisticated approaches for the separation of the metabolite signals. Furthermore, contributions of broad signals with short T_2 become increasingly apparent as an underlying "baseline" throughout the whole ^{1}H NMR spectrum (*6–9*).

A wealth of neurochemical information can be gained from high-resolution NMR spectroscopy. Identification and assignment of resonances has been performed, e.g., in perchloric acid extracts, extracted tissue, immobilized cells, and in animals and humans *in vivo* by 2D-H,C-HSQC, 2D COSY, *J*-resolved ^{1}H NMR experiments, and one-dimensional multinuclear approaches (*10–17*). *In vivo* ^{1}H NMR spectra have been quantified using several different approaches, such as time domain analysis combined with prior knowledge (*18*, *19*), frequency domain analysis (*20*), or combinations thereof (*21*), as well as principal component analysis, wavelet analysis, or genetic algorithms (*22–25*).

It has been recently demonstrated that the spectral resolution in ^{1}H NMR spectra *in vivo* increases significantly with static magnetic field, suggesting substantial improvements in sensitivity for the determination of previously unresolved signals (*26*). The purpose of the present study was to demonstrate that such gains can be realized in the rat brain *in vivo* at 9.4 T and to quantify the overall ^{1}H spectrum by LCModel analysis (*20*). Exploiting the improvements and stability recently achieved with a 1-ms echo time STEAM sequence (*27*), a further aim was to determine whether the underlying baseline resonances

[1] Abbreviations used: N-acetylaspartate, NAA; *N*-acetylaspartylglutamate, NAAG; alanine, Ala; γ-aminobutyric acid, GABA; aspartate, Asp; choline-containing compounds, Cho; coefficient of variation, CV; Cramér-Rao lower bounds, CR; creatine, Cr; echo time, TE; full width at half maximum, FWHM; glucose, Glc; glutamine, Gln; glutamate, Glu; glutathione, GSH; glycerophosphorylcholine, GPC; glycine, Gly; Hankel Lanczos singular value decomposition, HLSVD; *myo*-inositol, Ins; *scyllo*-inositol, Scyllo; lactate, Lac; macromolecule, MM; phosphocreatine, PCr; phosphorylcholine, PC; phosphorylethanolamine, PE; serine, Ser; signal to noise ratio, *S*/*N*; standard deviation, SD; taurine, Tau.

1090-7807/99 $30.00

can be ascribed entirely to macromolecule resonances with short T_1.

EXPERIMENTAL

Experiments were performed according to procedures approved by the Institutional Review Board's animal care and use committee. Male Sprague–Dawley rats (240–300 g, $n > 20$) were anesthetized by a gas mixture O_2:N_2O = 3:2 with 2% isofluorane. The rats were ventilated at physiological conditions by a pressure-controlled respirator (Kent Scientific Corp., Litchfield, CT). The oxygen saturation was maintained above 95% and was continuously monitored by a pulse oximeter attached to the tail (Nonin Medical, Inc., Minneapolis, MN). The body temperature was maintained at 37°C by warm water circulation and verified by a rectal thermosensor (Cole Parmer, Vernon Hills, IL). Femoral arterial and venous lines were used for regular blood gas analysis (P_{O_2}, P_{CO_2}, pH) and iv infusion of glucose, respectively.

All experiments were performed on a Varian INOVA spectrometer (Varian, Palo Alto, CA) interfaced to a 9.4-T magnet with 31-cm horizontal bore size (Magnex Scientific, Abingdon, UK). The actively shielded gradient coil insert (11-cm inner diameter) was capable of switching to 300 mT/m within 500 μs. Eddy current effects were minimized using methods and procedures described elsewhere (*28*). A quadrature surface RF coil consisting of two geometrically decoupled single-turn ^{1}H coils with 14-mm diameter, constructed according to a previously described design (*29*), was used for transmitting and receiving at 400 MHz proton frequency. To minimize the signal attenuation due to transverse relaxation (T_2) and *J*-modulation of coupled spin systems, the localization method was based on a 1-ms echo-time STEAM, described in detail elsewhere (*27*). Briefly, it was verified that the seven pulses of the VAPOR (variable pulse power and optimized relaxation delays) water suppression interleaved with outer volume saturation did not affect the M_z magnetization by more than 5% outside a region of $\pm$150 Hz ($\pm$0.38 ppm) of the water resonance. An adiabatic hyperbolic secant RF pulse (*30*) with 2-ms duration and 8-kHz inversion bandwidth was applied for inversion prior to the sequence to measure metabolite-nulled spectra. Adjustment of all first- and second-order shim terms was accomplished with a fully adiabatic version of FASTMAP (*26, 31*), resulting typically in an 11.5–13 Hz linewidth of the water resonance *in vivo* in a 5 $\times$ 2.5 $\times$ 5 mm voxel (63 μl). The voxel was positioned on the midline 2 mm posterior to bregma and 3 mm ventral. Routinely achieved linewidths of the singlet ^{1}H metabolite resonances were 8–10 Hz (0.02–0.025 ppm) *in vivo* and approximately 1 Hz (0.003 ppm) in phantoms.

Processing and Quantification

Interface software for data conversion and processing was written with PV-WAVE (Visual Numerics, Inc., Boulder, CO), which allowed automated frequency and phase correction and automated peak integration of the metabolite spectra. In some spectra the residual water signal was removed in the time domain using the Lanczos HLSVD routine (accelerated version of state-space HSVD) from the MRUI 97.1 software package (*32*).

Quantification was based on frequency domain analysis using LCModel (linear combination of model spectra of metabolite solutions *in vitro*, version 5.1–7W) (*20*). *In vivo* spectra were analyzed by a superposition of a set of *in vitro* basis spectra by means of a constrained regularization algorithm finding the best compromise between lineshape and baseline consistent with the data. The method uses the experimentally determined spectral pattern of each metabolite without further analysis.

In vitro spectra were collected from Ala, Asp, GPC, PC, Cr, PCr, GABA, Glc, Gln, Glu, GSH, Ins, Scyllo, Lac, NAA, NAAG, PE, and Tau. All chemicals were purchased from Sigma (St. Louis, MO). Aqueous solutions of 50 mM concentration of the metabolites were prepared in 100 mM phosphate buffer with 0.2 mM of 2,2-dimethyl-2-silapentane-5-sulfonate as the chemical shift reference (δ = 0.0 ppm). For choline-containing compounds the phosphate buffer was replaced by 100 mM sodium chloride. The pH was adjusted to 7.10, and temperature was maintained at 37°C by warm water circulation using a heating blanket and verified by a thermosensor.

In vivo spectra were referenced to the methyl signal of NAA (δ = 2.009 ppm) and the inversion recovery spectra to the macromolecule M1 resonance (δ = 0.916 ppm). *In vitro* model spectra were calibrated by integrating the ^{1}H metabolite resonances and by adjusting the nominal concentrations for the LCModel input. *In vivo* metabolite concentrations were determined using the intensity of the water signal measured at echo time TE = 2 ms as an internal standard and assuming a constant tissue water content of 83% for the rat brain (*33*) and a 100% visibility of the water signal. This procedure accounted for different voxel sizes, spatial variation of sensitivity of the surface coil, and different coil loadings. Metabolite concentrations were expressed as micromoles per gram wet weight (ww). The effect of potential animal motion on the summed signal was assessed to be below 0.5% by measuring the phase and amplitude stability of single-shot water signals. In the LCModel fit, only a zero-order phase correction was performed resulting from proper timing of the first sampled data point in the pulse sequence. Eddy-current effects were minimal and the field drift was less than 1 Hz. An extended spectral range for LCModel's finite discrete convolution was chosen to account for the *in vivo* Lorentzian lineshape with long tails due to the very good shimming.

RESULTS

^{1}H NMR spectra of the rat brain *in vivo* with 2-ms echo time were analyzed with LCModel including 18 metabolite model

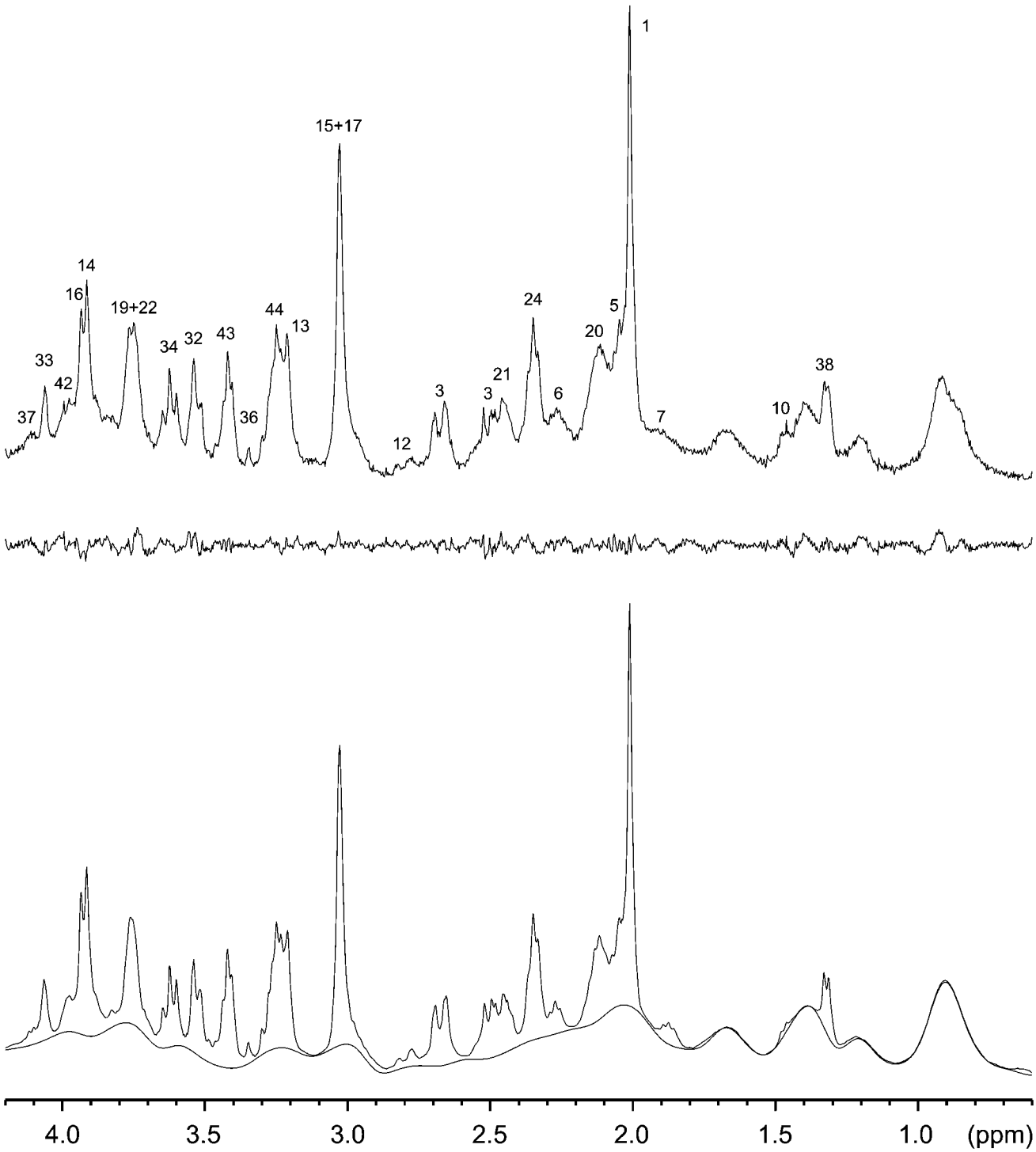

FIG. 1. LCModel analysis of a short-echo-time ^{1}H NMR spectrum of the rat brain *in vivo* including 18 metabolite model spectra (TE = 2 ms, TM = 20 ms, TR = 6 s, 512 scans, 63-μL volume). Shown is the *in vivo* spectrum (top), the fitted spectrum with spline baseline (bottom), and the residuals (middle trace). The assignment of the peaks corresponds to the numbers in Table 1. Only FT and zero-order phase correction was applied (no weighting function).

spectra. In Fig. 1 the measured and fitted spectrum are shown together with the residuals and the spline baseline as determined by LCModel. The numbers indicate more than 40 detected resonances, which are assigned in Table 1. Although the determined metabolite concentrations were consistent with previous neurochemical measurements and had reasonable errors, a significantly varying baseline remained, despite excellent water suppression and suppression of signals from outside the

TABLE 1
^{1}H Chemical Shifts of Cerebral Metabolites, Detected in Rat Brain *in Vivo* Corresponding to Fig. 1

No.	Compound		Carbon position	^{1}H chemical shift	
				in vivo spectra (ppm)	Fitted model spectra (ppm)
1	*N*-Acetylaspartate	CH_3		2.009 (Ref.)	
2		αCH	C2		4.377
3		βCH_2	C3	2.489 + 2.674	
4		NH		7.82	
5	*N*-Acetylaspartylglutamate	CH_3		2.046	
6	γ-Aminobutyric acid	αCH_2	C2	2.28	
7		βCH_2	C3	1.89	
8		γCH_2	C4		3.01
9	Alanine	αCH	C2		3.777
10		βCH_3	C3	1.468	
11	Aspartate	αCH	C2		3.88
12		βCH_2	C3	2.79	2.66 + 2.79
13	Choline compounds	$(CH_3)_3$		3.209	
14	Creatine	CH_2		3.911	
15		CH_3		3.027	3.024
16	Phosphocreatine	CH_2		3.931	
17		CH_3		3.027	3.030
18	α-Glucose	[1]CH	C1	5.226	
19	Glutamine	αCH	C2		3.76
20		βCH_2	C3	2.12	
21		γCH_2	C4	2.45	
22	Glutamate	αCH	C2	3.75	
23		βCH_2	C3		2.08
24		γCH_2	C4	2.349	
25	Glutathione	Gly CH + Glu αCH	C2		3.77
26		Glu βCH_2	Glu C3		2.16
27		Glu γCH_2	Glu C4		2.54
28		Cys βCH_2	Cys C3		2.95
29	Glycerophosphorylcholine	NCH_2 + Glyc CH_2			3.66
30		OCH_2			4.31
31		Glyc OCH_2 + CH			3.90
32	*myo*-Inositol	[1,3]CH	C1,C3	3.525	
33		[2]CH	C2	4.060	
34		[4,6]CH	C4,C6	3.622	
35		[5]CH	C5	3.275	
36	*scyllo*-Inositol	CH		3.345	
37	Lactate	αCH	C2	4.11	
38		βCH_3	C3	1.318	
39	Phosphorylcholine	NCH_2			3.58
40		OCH_2			4.16
41	Phosphorylethanolamine	NCH_2			3.22
42		$POCH_2$		3.98	
43	Taurine	SCH_2		3.418	
44		NCH_2		3.246	

Note. ^{1}H chemical shifts were referenced to the *N*-acetylaspartate methyl peak. The assignment was based on LCModel analysis containing model solution spectra. Chemical shifts were determined from peak positions *in vivo* and from the fitted model spectra with an accuracy of ±1 Hz (±0.003 ppm).

volume of interest. The apparent structure of the spline baseline suggested the presence of biological signals underlying the narrow metabolite peaks, consistent with previous reports of large molecular weight compounds contributing to the spectrum of brain extracts (*14*) with relatively short T_1 and T_2 compared with acid-extracted metabolites. We therefore further assessed potential macromolecule contributions to the *in vivo* spectrum and the effect on the quantification of including a measured macromolecule spectrum to the LCModel approach.

TABLE 2

T_1 and T_2 Relaxation Times and Corresponding Inversion Recovery Times at Which M_z is Zero (t_{IR}^{null}) in the Rat Brain *in Vivo* at 9.4 T

	t_{IR}^{null} (s)	T_1 (s)	T_2 (ms)
N-acetylaspartate CH_3 (2.009 ppm)	0.98 ± 0.01	1.41 ± 0.02	144 ± 7
Creatine/phosphocreatine CH_3 (3.025 ppm)	0.93 ± 0.02	1.34 ± 0.03	104 ± 4
Choline compounds CH_3 (3.206 ppm)	0.95 ± 0.03	1.37 ± 0.04	147 ± 10
Creatine/phosphocreatine CH_2 (3.916 ppm)	0.61 ± 0.02	0.88 ± 0.03	91 ± 7

Note. T_1 and t_{IR}^{null} were fitted from the data shown in Fig. 2. To determine T_2, the echo time was varied by TE = 100–200 ms (increment 10 ms) and peak integrals were fitted by log-linear regression.

Baseline in ^1H Spectra

T_1 values of rat brain metabolites *in vivo* at 9.4 T (Table 2) were determined from the inversion recovery experiment shown in Fig. 2. To minimize confounding effects of the underlying macromolecule (MM) resonances with shorter T_2, the echo time (TE) was set to 100 ms. The signals of the NAA, Cr + PCr, and Cho methyl peaks as well as those from Tau were minimized when the inversion time t_{IR} was between 0.93 and 0.98 s, whereas the Cr + PCr methylene resonances were minimized at the significantly shorter t_{IR} of 0.61 s. The T_2 values for these metabolites were fitted by log-linear regression of a series of 11 spectra acquired with equally spaced echo times between 100 and 200 ms (data not shown), resulting in T_2 values between 91 and 147 ms (Table 2).

To determine the macromolecule contributions in short-echo-time spectra *in vivo*, the nulling time after the inversion pulse, t_{IR}^{null}, was set to 0.95 s according to Table 2. The spectra acquired with TE = 2 ms and TE = 20 ms using this t_{IR}^{null} (Fig. 3) represent mostly macromolecule signals which have been reported with short T_1 (*14*). Major resonances were observed at 0.916 ppm (labeled M1, which was used as reference), 1.21 (M2), 1.39 (M3), 1.67 (M4), 2.04 (M5), 2.26 (M6), and 2.99 ppm (M7). In addition, we also consistently observed resonances at 3.21 (M8), 3.77 (M9), and 4.29 ppm (M10). When increasing TE to 20 ms these macromolecule signals were reduced by approximately 50% relative to TE = 2 ms (bottom spectrum in Fig. 3). Note that the narrow peak at 3.925 ppm was assigned to the incompletely suppressed Cr + PCr methylene resonances, for which T_1 was 40% reduced compared to the other metabolites (Table 2). The T_2 of the macromolecule signals, T_2^{MM}, was estimated from the two spectra shown in Fig. 3 to be approximately 26 ms. T_1 of the resolved macromolecule peaks, T_1^{MM}, was estimated from an inversion recovery experiment (t_{IR} = 160–340 ms) to be approximately 300 ms (data not shown). Both relaxation times were three to six times shorter than those of the metabolites, which can be used for a separation of signals based on the different relaxation properties.

To further minimize contributions from metabolite signals to the spectrum with t_{IR}^{null} = 0.95 s, the Cr + PCr methylene resonance was eliminated in the time domain using HLSVD analysis and by applying exponential multiplication corresponding to a linebroadening of 20 Hz. The residual contribution of metabolite signals with the T_1 in the range of 1.32–1.42 s was estimated to be ±2% of the fully recovered intensity and the effect on quantification was therefore considered negligible.

The MM basis spectrum, used for the analysis of the 2-ms echo-time ^1H spectrum in Fig. 1, is shown in Fig. 4 (solid curve) and compared to the spline baseline of Fig. 1 obtained when the MM spectrum was omitted from the basis set (dashed curve). The default minimal knot spacing of 0.1 ppm for the LCModel regularized spline baseline allowed enough flexibility at most spectral resolutions, *S*/*N*, and TE. To account for the rapidly varying baseline (Fig. 4, dashed curve), the minimal

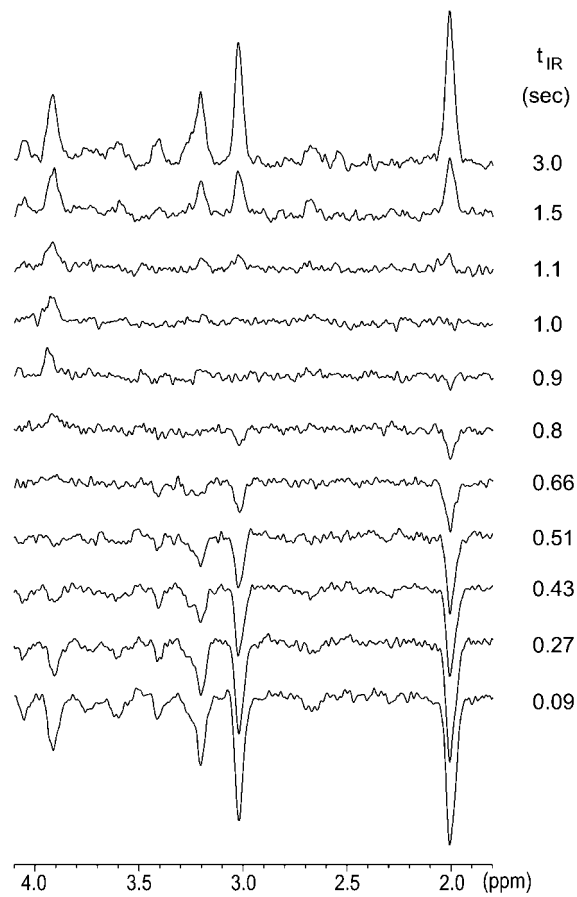

FIG. 2. Series of ^1H NMR spectra with differing inversion-recovery times (t_{IR}) for determination of the T_1 values of metabolites (TE = 100 ms, TM = 20 ms, TR = 4 s). Nearly all metabolite signals are nulled at $t_{IR} \sim 1.0$ s with the exception of the Cr + PCr resonances at 3.92 ppm, which have shorter T_1 that are nulled at $t_{IR} \sim 0.66$ s. The estimated T_1 values are given in Table 2.

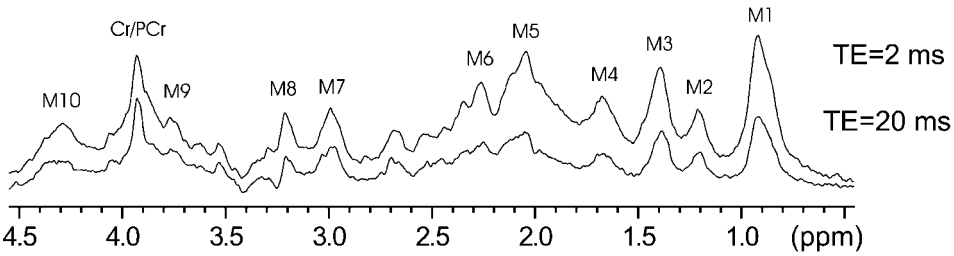

FIG. 3. *In vivo* metabolite-nulled ^{1}H NMR spectra in the rat brain, obtained at TE = 2 and 20 ms. The inversion-recovery time t_{IR}^{null} was set to 950 ms. Macromolecule resonances are labeled by M1 (0.916 ppm, reference), M2 (1.21), M3 (1.39), M4 (1.67), M5 (2.04), M6 (2.26), and M7 (2.99) according to Ref. (*14*) and are extended by M8 (3.21), M9 (3.77), and M10 (4.29). Due to faster relaxation (see Fig. 2), the creatine and phosphocreatine methylene resonance at 3.93 ppm with the distinct narrow linewidth was not completely eliminated. The spectra were processed with 6 Hz Lorentzian linebroadening.

spacing was further reduced to 0.05 ppm, based on the linewidth of the macromolecule peak M1 (approximately 0.1 ppm). When the MM spectrum was included in the basis set, the minimal knot spacing was increased to 0.25 ppm. As can be seen from Fig. 4 (solid curve), the spline baseline mimicked the MM peaks very well. *In vivo*, inclusion of the MM basis spectrum consistently flattened and reduced the residual spline baseline substantially.

The comparison of the experimentally based MM background to the fitted spline baseline shown in Fig. 4 demonstrates that the latter reproduces the MM spectrum very well for the resolved macromolecule peaks M1–M4 as well as M5, M7, and M8 underneath the NAA, Cr + PCr, and Cho methyl peaks. However, even with a tight knot spacing of 0.05 ppm, the spline baseline could not completely reproduce all features of the *in vivo* MM spectrum. For example, a significant underestimation was observed at M6 (2.26 ppm) and around 1.9 ppm, which led to a 230% overestimated GABA concentration. Likewise M5, M7, and M8 were underestimated leading to slightly higher concentrations of NAA, Cr, and Cho. Overall, the concentrations and corresponding Cramér–Rao (CR) lower bounds tended to be approximately 6% higher when using the spline baseline only.

Quantification and Assignment in Short-Echo-Time Spectra

The *in vivo* ^{1}H NMR spectrum of Fig. 1 was analyzed with the 18 metabolite solution spectra and an *experimentally* determined macromolecule model spectrum (Fig. 5). Quantitative results are shown in Table 3 together with comparative neurochemical data from the literature (*13, 33–40*). The comparison of the *in vivo* with the fitted data (TE = 2 ms) shows that the solution model metabolite spectra (with a long T_1) together with the MM spectrum (short T_1) account for most spectral features (Fig. 5). The contributions of alanine (1.47 ppm) and lactate (1.32 ppm) are shown in the upfield region <1.8 ppm, which is otherwise dominated by macromolecule resonances. To allow a detailed comparison of the solution spectra and their quantitative contributions to the *in vivo* spectrum, five different traces are shown in Fig. 6. Covering the spectral range of 4.2–1.8 ppm includes resonances from NAA, Cr, PCr, Tau, and glycerophosphorylcholine + phosphorylcholine (GPC + PC) (second trace), Ins, Gln, Glu, Lac, Scyllo, and NAAG (third trace), Glc (fourth trace), and phosphorylethanolamine (PE), GSH, GABA, and Asp in the bottom trace.

Figure 6 demonstrates that most of the 18 metabolites gave rise to unique and identifiable peaks in the rat brain spectrum *in vivo* at 9.4 T. The creatine and phosphocreatine methylene peaks were resolved at 3.911 and 3.931 ppm, and the ratio [Cr]/[PCr] was approximately 1.2. A small difference in the Cr and PCr methyl chemical shift at 3.027 ppm resulted in an approximately 2-Hz larger linewidth compared to the NAA methyl singlet at 2.009 ppm. The taurine methylene resonance at 3.418 ppm revealed a spectral pattern (triplet) that closely resembled the model spectrum of Tau, suggesting that contri-

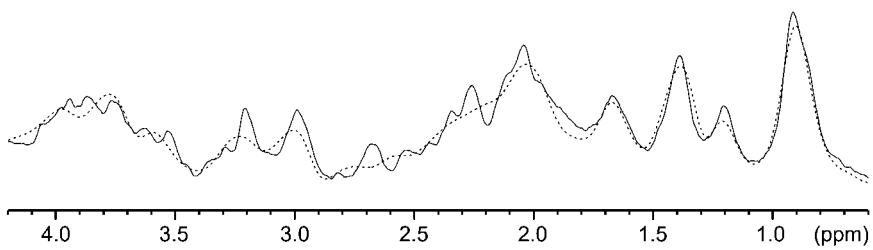

FIG. 4. Comparison of the LCModel spline baseline (dashed curve) and the measured metabolite-nulled spectrum (Figs. 1 and 5). The agreement of the spline with the experimental macromolecule spectrum is excellent despite the fact that no prior knowledge has been included in the spline baseline. The main differences of the spline are smoothing at positions 3.2, 3.0, 2.7, 2.25, 2.0, and 1.9 ppm, which may lead to an overestimation of NAA, Cr, Cho, and GABA concentrations compared to the inclusion of a macromolecule basis spectrum in the analysis.

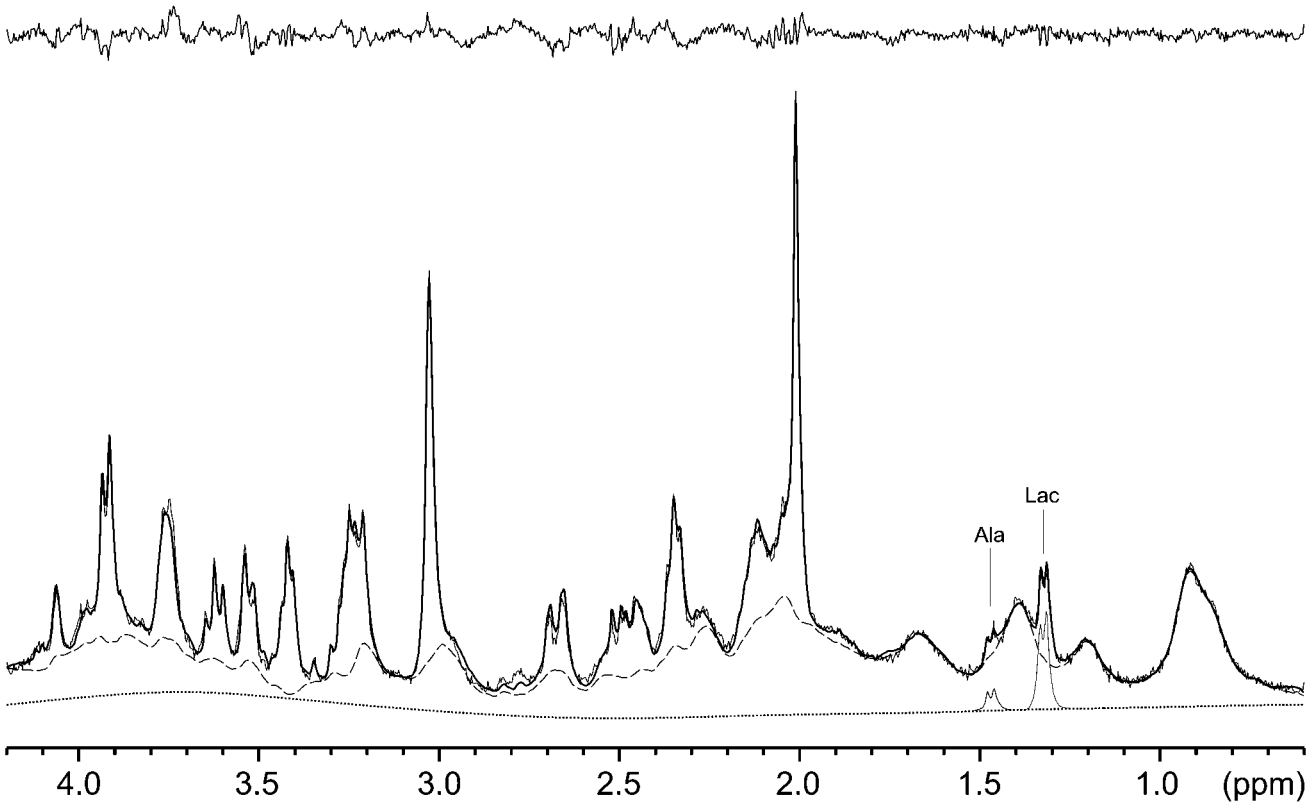

FIG. 5. LCModel analysis of a short-echo-time ^{1}H NMR spectrum of the rat brain *in vivo* (TE = 2 ms, TM = 20 ms, TR = 6 s, same data as in Fig. 1). Shown is the spectrum (thin solid curve), the fit (thick solid curve), the fitted macromolecule spectrum (dashed curve), and the residuals (top). In the spectral region from 1.8 to 0.7 ppm, containing mostly macromolecule resonances, the fitted contributions of alanine and lactate are shown. Note the slowly varying spline baseline (dotted curve).

butions from other compounds such as glucose at 3.4 ppm contribute minor spectral features to that region. The coupling pattern, relative intensities, and frequencies of the *myo*-inositol resonances were in excellent agreement with the model spectrum. A highly structured pattern of the NAA signals was discernible at 2.489 and 2.674 ppm corresponding to the two magnetically nonequivalent βCH_2 protons. Several peaks were recognized in the region 3.3–3.2 ppm, which were explained by contributions from Tau, Ins, Glc, and PE that could be deconvoluted from the choline methyl peak of GPC + PC at 3.209 ppm. The concentration ratio of NAA relative to total creatine was [NAA]/[Cr + PCr] = 1.05 and [GPC + PC]/[Cr + PCr] = 0.06.

It is noteworthy that the γCH_2 resonances of glutamate and glutamine at 2.35 and 2.45 ppm were completely resolved *in vivo*. Furthermore, the βCH_2 resonances of glutamate and glutamine at 2.08 and 2.12 ppm indicated a distinct spectral pattern (TE = 2 ms, TM = 20 ms). The C1 resonance from α-glucose was routinely detected downfield at 5.226 ppm and other glucose contributions in the regions at 3.95–3.65 and 3.55–3.35, as well as at 3.25 ppm. In addition, *scyllo*-inositol, NAAG, GABA αCH_2, and βCH_2 at 2.28 and 1.89 ppm, aspartate βCH_2 at 2.79 ppm, and lactate αCH at 4.11 ppm gave rise to discernible spectral features.

A feature of ^{1}H NMR spectra acquired from the dog and rat brain *in vivo* at 9.4 T was a partially resolved peak at 3.98 ppm (*26*, *27*). In that region, PE has coupled signals as does serine (Ser) (Fig. 7). The resolution-enhanced rat brain *in vivo* spectrum in Fig. 8 showed that the spectral pattern of PE with resonances at 3.98 and 3.22 ppm matched the *in vivo* spectrum between the Ins (4.060 ppm) and the PCr and Cr (3.931, 3.911 ppm) peaks with respect to chemical shift and lineshape (second trace). In contrast, Ser had resonances at 3.98–3.94 and 3.83 ppm (third trace in Fig. 7). Nearby peaks from Lac, PCr, Cr, Gln + Glu, Scyllo, and GPC + PC had clearly different resonance positions. When both PE and Ser were included in the LCModel analysis, concentrations of PE were 1.5–1.7 μmol/g ww (CR = 8–11%) and concentrations of Ser were 0.2–0.6 μmol/g ww (CR = 41–73%). Because Ser concentrations were much less consistent and found with a high CR error, a major contribution of Ser was not evident and thus Ser was omitted from the set of model spectra.

The strongly represented metabolites NAA, Cr, PCr, Tau, Ins, Glu, Gln, and Lac were estimated with Cramér–Rao lower

TABLE 3
Metabolite Concentrations in the Rat Brain *in Vivo* Resulting from an LCModel Analysis of a Short-Echo-Time ^{1}H NMR Spectrum at TE = 2 ms, TM = 20 ms, TR = 6 s (Fig. 5)

	Present study[a]			Neurochemical literature data	
	Concentration (μmol/g ww)	Relative to [Cr + PCr]	CR (%)	Concentration (μmol/g ww)	Reference
Ala	0.55	0.06	13	0.32, 0.14–0.94, 0.48, 0.65, 0.40	(*13*, *33–35*, *37*)
Asp	0.90	0.11	22	2.32, 1.53–2.72, 2.78, 2.60, 2.46, 2.67	(*13*, *33–37*)
GPC	0.15	0.02	40		
PC	0.35	0.04	16	0.5	(*33*)
GPC + PC	0.50	0.06	6		
Cr	4.7	0.55	2	4.91, 5.12	(*13*, *36*)
PCr	3.9	0.45	3	3.43, 3.2–5.0, 4.05	(*13*, *33*, *36*)
Cr + PCr	8.5	1.0	1		
GABA	0.77	0.09	12	1.62, 0.83–2.27, 1.90, 2.30, 1.99	(*13*, *33–35*, *37*)
Glc	2.7	0.31	8	0.96	(*36*)
Gln	2.7	0.32	4	2.15–5.60, 5.02, 4.50, 5.59	(*33–35*, *37*)
Glu	8.3	0.97	2	7.43, 7.81–12.5, 12.46, 11.60, 11.2, 12.0	(*13*, *33–37*)
GSH	0.78	0.09	9	0.90–3.40, 2.23, 2.60	(*33–35*)
Gly	n.d.	n.d.	n.d.	0.64, 0.55–1.46, 1.02, 0.68, 1.00	(*13*, *33–35*, *37*)
Ins	4.4	0.51	2	10.5	(*13*)
Scyllo	0.16	0.02	20		
Ser	n.d.	n.d.	n.d.	0.39–1.77, 0.86, 0.98, 0.88	(*33–35*, *37*)
Lac	2.8	0.33	3	1.16, 1.23	(*13*, *36*)
NAA	8.9	1.05	1	5.99, 4.70–9.74, 5.60	(*13*, *33*, *35*)
NAAG	0.54	0.06	13	0.030–0.074 relative to [NAA]	(*38*)
GPE	n.d.	n.d.	n.d.	0.43	(*34*)
PE	1.7	0.20	6	1.5, 1.36, 2.00	(*33–35*)
Tau	6.0	0.70	2	1.66, 1.25–5.35, 4.60, 6.60, 5.49	(*13*, *33–35*, *37*)

[a] FWHM = 0.026 ppm, S/N = 45, Cramér–Rao lower bounds (CR) are given in percentages.

bounds below 4%, weaker metabolites below 13%, e.g., 6% for GPC + PC, 6% for PE, 8% for GSH, and 12% for GABA, and Asp and Scyllo below 22% (see Table 3 for a detailed listing).

An analysis of a spectrum with increased TE = 20 ms but otherwise identical experimental conditions is shown in Fig. 8. Due to T_2 relaxation, an overall decreased intensity of the metabolites and the macromolecule resonances was discernible. In addition, *J*-modulation led to an altered spectral appearance compared to TE = 2 ms (Fig. 6) that was very well reproduced by the model solution spectra for, e.g., NAA and ASP.

To assess the influence of the echo time TE and repetition time TR on the quantification, the LCModel results of three different measurements were compared with (A) TE = 2 ms, TR = 6 s, (B) TE = 20 ms, TR = 6 s, and (C) TE = 20 ms, TR = 4 s. Increasing TE from 2 to 20 ms with the same TR decreased the concentrations of total creatine, [Cr + PCr], by 6%, [NAA] by 4%, and on average over all metabolites by 4%. Decreasing TR from 6 to 4 s further decreased the concentrations of [Cr + PCr] by an additional 6%, [NAA] by 7%, and on average by 5%. However, the ratio [NAA]/[Cr + PCr] remained constant within 3%, reflecting the similar relaxation times of creatine and NAA. The average concentration correction factor due to the T_2 relaxation at TE = 2 ms was estimated to be less than 1%, which was well within the experimental variation.

Reproducibility

The error estimates from the standard least-squares covariance matrix (Cramér–Rao lower bounds (*20*)) are lower bounds of the experimental variance because they are based on several assumptions. The most critical assumption is that the model is correct (or at least contains sufficient parameters to describe the data within experimental error). For instance, the Cramér–Rao lower bounds can be unrealistically low for insufficiently parameterized models.

Therefore, a direct experimental measure of the precision of the estimates, the intra-assay variation, was determined with a time series (1 h 45 min total measurement time) acquired with 32 blocks of 3-min acquisitions each using TE = 20 ms and TR = 6 s to compare the Cramér–Rao lower bounds with the standard deviation of the series. Table 4 shows that the coefficients of variation (CV) of the strongly represented metabolites (PCr, Cr, Glu, Ins, NAA, Tau) were below 5%, and for the weaker metabolites (GPC + PC, Glc, Gln, GSH, Lac, PE) below 12%. The CV were in excellent agreement with the Cramér–Rao lower bounds for a single 3-min spectrum (32

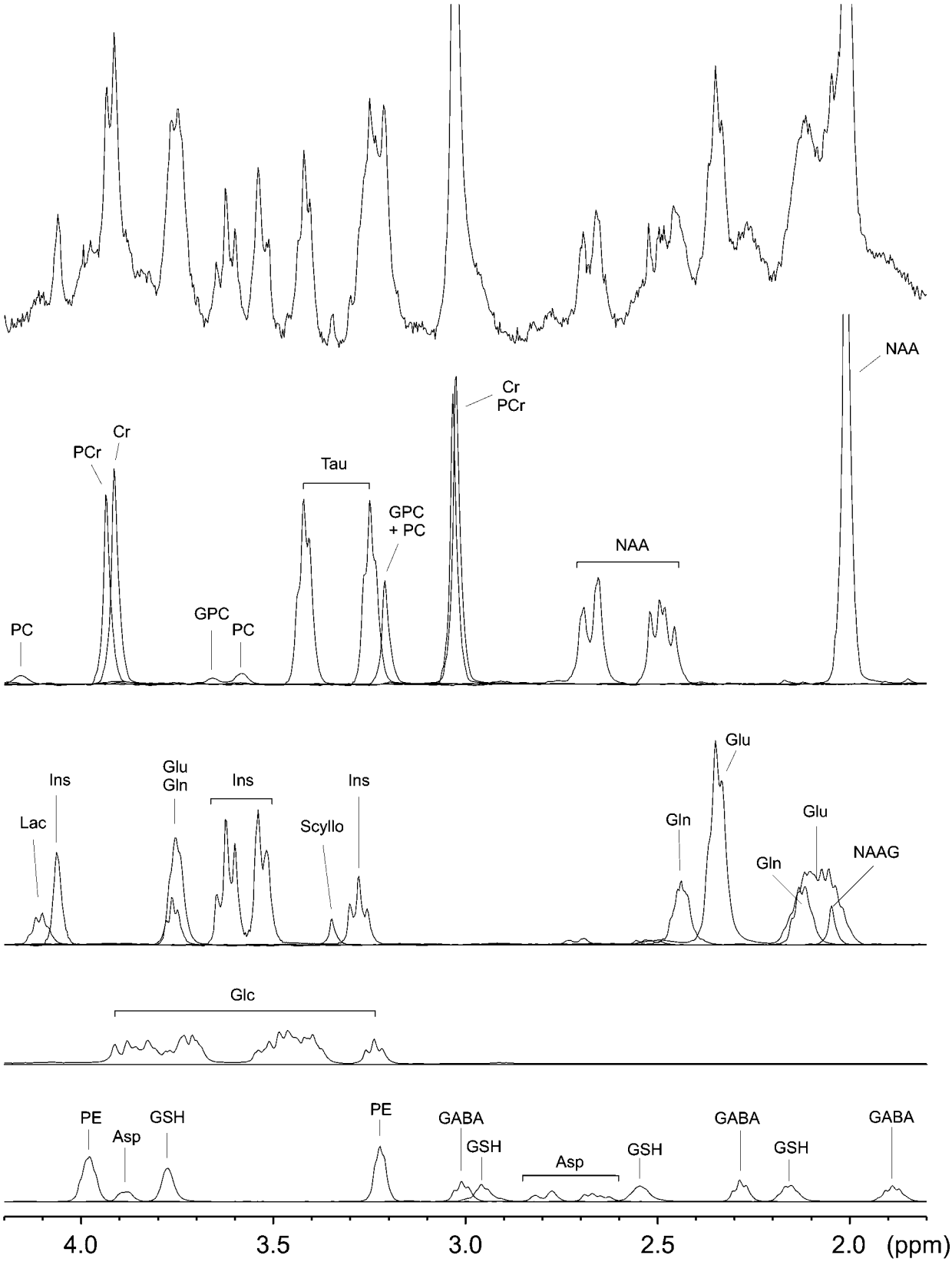

FIG. 6. Comparison of the *in vivo* ^{1}H NMR spectrum of Fig. 5 (top) to ^{1}H NMR metabolite model spectra (TE = 2 ms, TM = 20 ms, TR = 6 s, 512 scans, 63-μL volume). Quantitative results are shown in Table 3. Only FT and zero-order phase correction was applied to the *in vivo* data (no weighting function).

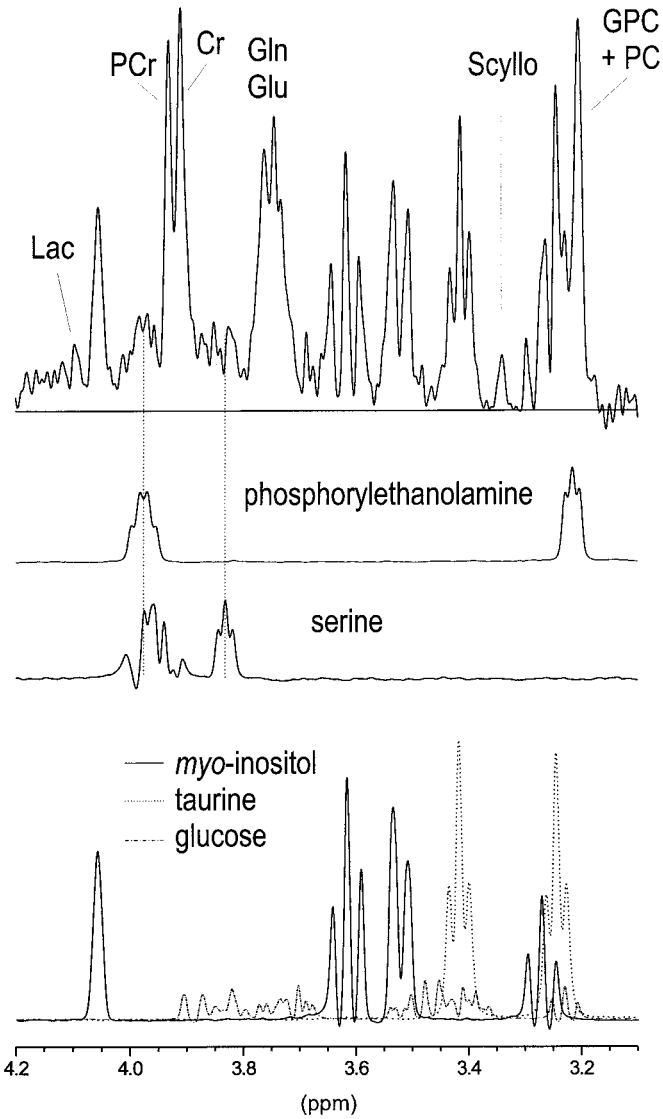

FIG. 7. Resolution-enhanced ^{1}H NMR spectrum of the rat brain *in vivo* in the spectral region from 4.2 to 3.1 ppm (TE = 20 ms, same data as in Fig. 8, shifted sine-bell function). Model solution spectra of phosphorylethanolamine, serine, *myo*-inositol, taurine (dotted), and glucose (dashed) were processed with 2 Hz Gaussian linebroadening. The spectral patterns are in excellent agreement with the *in vivo* data with the exception of serine. Peak separation of PCr and Cr can be recognized at 3.9 ppm. The contributions of *myo*-inositol-, taurine-, and choline-containing compounds are clearly discernible at 3.3–3.2 ppm.

scans), i.e., 2% for NAA, 7% for Cr, 6% for PCr, 4% for Glu, 4% for Ins, and 6% for Tau. The fact that CR are very close to CV suggests that our model closely approximates the information content of the *in vivo* situation. When averaging four 3-min spectra (128 scans), the errors were reduced approximately twofold, as can be seen in column 5 of Table 4. In these 13-min spectra, most metabolites were detected with a CV below 8%, and variation of total creatine was on the order of 1%. The accuracy of several weak metabolites was also significantly improved, i.e., CV was 11% for Scyllo, 14% for GABA, 18% for Ala, and 26% for Asp.

The interassay reproducibility was determined by analyzing spectra measured under similar conditions, whereby experimental parameters were chosen to be TE = 20 ms and TR = 4 s to facilitate comparison with other studies at short echo times. Deliberately, all 31 spectra acquired from 20 animals were used without exclusions. A wide range of linewidth (FWHM = 0.025–0.041 ppm) and signal-to-noise ratio (S/N = 18–38) was, therefore, present in the data. To compare with previous analyses in Refs. (*19, 41*) and to reduce uncertainties of the quantification, concentrations were determined relative to the total creatine concentrations. The experimentally determined average value was 7.78 μmol/g ww (CV = 7.4%, relative to water at TE = 2 ms), which was not corrected for T_1 and T_2 and thus underestimates the true concentration by at least 10%. The coefficients of variation for NAA, Glu, Cr, PCr, GSH, and PE were below 10%, and for Ins, Glc, Tau, GPC + PC, Lac, and Ala below 20% (Table 5), demonstrating the consistency and robustness of the LCModel analysis. The reliability was much higher in the analysis of higher quality spectra using 2-ms echo time, such as those shown in Figs. 5 and 6, with excellent shimming (FWHM = 0.026 ppm), and high signal-to-noise ratio (S/N = 45).

To assess the influence of the quality of shimming on metabolite determinations, the linewidths were artificially increased by applying additional exponential multiplication to the FID before the LCModel analysis. Progressive linebroadening of the 2-ms echo-time ^{1}H spectrum (Fig. 5) from 0 to 30 Hz decreased the correlation coefficient between Cr and PCr linearly from −0.71 to −0.92, thus demonstrating the increasing difficulty of distinguishing Cr from PCr. The correlation coefficient of GPC and PC without additional linebroadening was −0.87, which is already close to −1. When linebroadening was applied, GPC was not detectable any more, suggesting that the concentrations of GPC and PC were difficult to determine separately, but the sum [GPC + PC] remained highly reliable (see Table 3).

Applications: Hyperglycemia and Hepatic Encephalopathy

To quantify the glucose concentration in the rat brain, the spectral region of the LCModel analysis was extended through the water region to 5.4 ppm to include the α-Glc [1]CH resonance at 5.226 ppm. Hyperglycemia was induced by infusion of glucose at a constant rate of 4 mg/min. The comparison of the *in vivo* ^{1}H NMR spectrum with the fitted glucose spectrum (Fig. 9) shows that in addition to the resonance at 5.226 ppm, partially resolved peaks at 3.87, 3.83, 3.49, and 3.46 ppm (dotted lines) from the Glc spectrum were discernible. A small water peak that remained after water suppression (dashed curve) was fitted by HLSVD and removed in the time

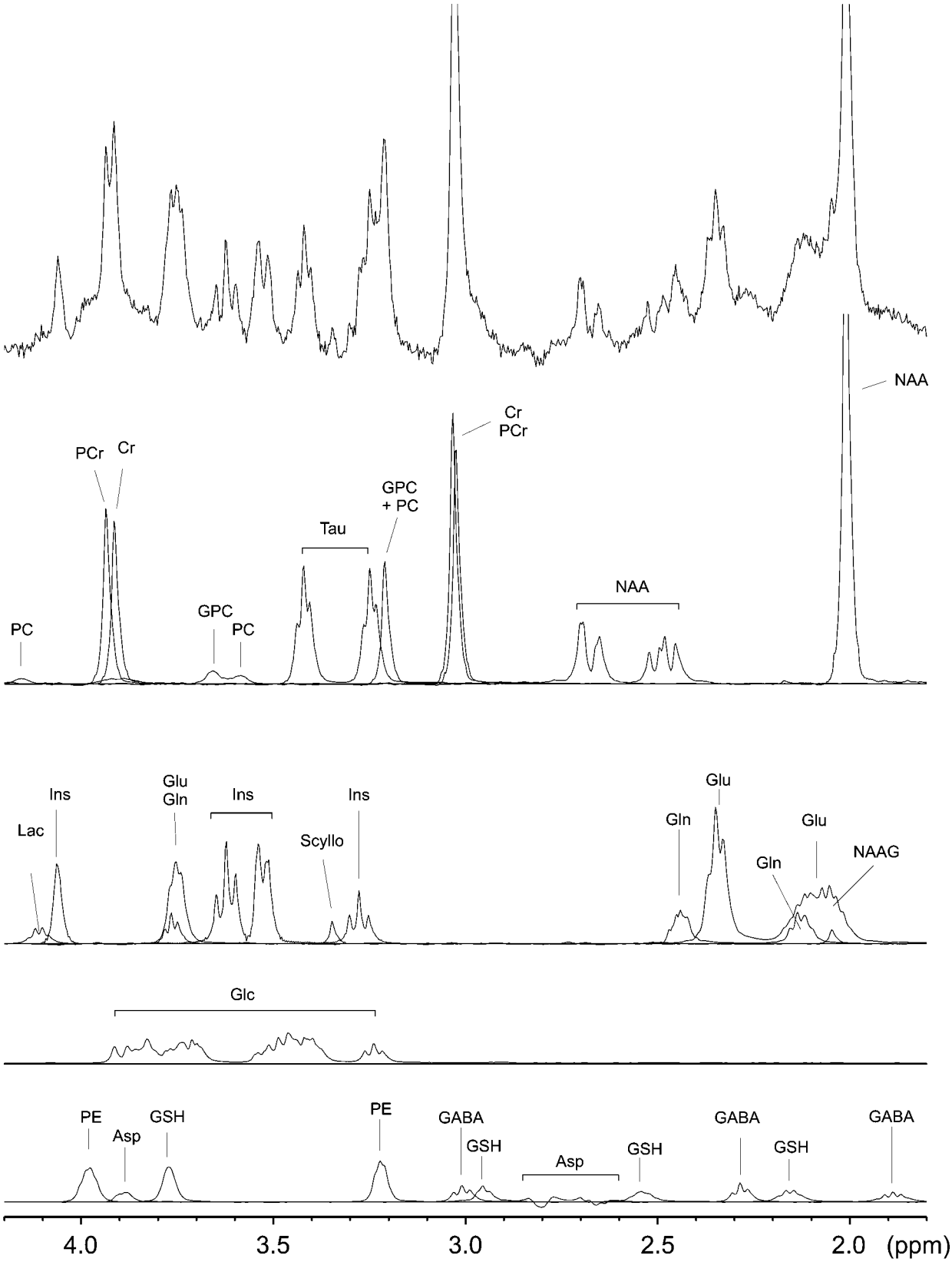

FIG. 8. *In vivo* ^{1}H NMR spectrum from the same animal and voxel as in Fig. 6, but at longer echo time TE = 20 ms. The signal intensity is significantly decreased compared to Fig. 6 due to T_2 relaxation. The spectral pattern, e.g., of NAA or Asp βCH_2 resonances, is altered due to *J*-evolution.

domain to keep the residual around the water region low. The Glc concentration in this spectrum was 5.2 μmol/g ww (CR = 4%). An LCModel analysis that did not include the α-Glc C1 resonance at 5.226 ppm yielded the same result within 2%, consistent with the detection of several discernible glucose resonances in the upfield side of the spectrum at 9.4 T. In addition, after progressively linebroadening from 0 to 30 Hz of the hyperglycemic rat spectrum, the LCModel analysis did not reveal a significant difference whether the α-Glc C1 resonance at 5.226 ppm was included, but a general decrease in the concentration was observed unless the concentration was referenced to Cr + PCr.

A ^{1}H NMR spectrum with 2-ms echo time of a pathological rat brain is shown in Fig. 10 as an example of quantification of elevated glutamine (*26*, *42*). Glutamine was increased threefold compared to normal brain (7.2 μmol/g ww, CR = 2%), whereas *myo*-inositol (2.1 μmol/g ww, CR = 6%) and choline-containing compounds GPC + PC (0.31 μmol/g ww, CR = 13%) were decreased by approximately 50%. All other metabolites, including glutamate, were in the range of the values measured from the healthy rat brain shown in Table 3.

TABLE 4
Intra-assay Variation of Metabolite Concentrations in a Series of ^{1}H NMR Spectra of the Healthy Rat Brain *in Vivo*

	3-min spectra		13-min spectra	
	Mean ± SD (μmol/g ww)	CV (%)	Mean ± SD (μmol/g ww)	CV (%)
Ala	0.48 ± 0.14	30	0.48 ± 0.09	18
Asp	1.00 ± 0.43	43	1.03 ± 0.27	26
GPC	0.36 ± 0.11	31	0.34 ± 0.04	13
PC	0.17 ± 0.10	57	0.19 ± 0.03	15
GPC + PC	0.54 ± 0.04	8.2	0.53 ± 0.03	5.7
Cr	4.15 ± 0.21	5.0	4.19 ± 0.13	3.1
PCr	3.95 ± 0.16	4.0	3.79 ± 0.05	1.4
Cr + PCr	8.10 ± 0.14	1.8	7.98 ± 0.09	1.1
GABA	0.76 ± 0.25	33	1.02 ± 0.14	14
Glc	4.14 ± 0.36	8.7	3.39 ± 0.26	7.8
Gln	2.27 ± 0.28	12	2.44 ± 0.11	4.4
Glu	8.36 ± 0.33	4.0	8.61 ± 0.15	1.8
GSH	1.24 ± 0.15	12	1.12 ± 0.07	6.0
Ins	4.69 ± 0.20	4.3	4.42 ± 0.05	1.2
Scyllo	0.20 ± 0.06	27	0.17 ± 0.02	11
Lac	2.90 ± 0.22	7.4	2.85 ± 0.18	6.5
NAA	8.50 ± 0.15	1.8	8.62 ± 0.13	1.5
NAAG	0.20 ± 0.11	57	0.22 ± 0.08	38
PE	2.00 ± 0.24	12	1.91 ± 0.12	6.1
Tau	4.98 ± 0.24	4.8	5.05 ± 0.10	1.9

Note. The concentrations were not corrected for T_2-related signal decay. Spectra were acquired from one animal during an overall 105-min experiment (TE = 20 ms, TM = 20 ms, TR = 6 s). Blocks of 32 and 128 scans were analyzed with LCModel and the concentrations were averaged (S/N = 20 and 35).

TABLE 5
Interassay Variation of Metabolite Concentrations of 31 ^{1}H NMR Spectra from 20 Animals Analyzed by LCModel (TE = 20 ms, TM = 20 ms, TR = 4 s)

	Pooled rat data		
	Mean ± SD (μmol/g ww)	CV (%)	Number of spectra
Ala	0.31 ± 0.06	20	(n = 22)
Asp	1.43 ± 0.44	30	(n = 7)
GPC	0.33 ± 0.11	34	(n = 15)
PC	0.61 ± 0.10	16	(n = 30)
GPC + PC	0.71 ± 0.10	14	
Cr	3.86 ± 0.33	9	
PCr	3.92 ± 0.33	9	
Cr + PCr	7.78		
GABA	1.11 ± 0.25	22	
Glc	3.51 ± 0.46	13	(n = 10)[a]
Gln	1.25 ± 0.38	30	
Glu	8.67 ± 0.70	8	
GSH	1.46 ± 0.15	10	
Ins	4.08 ± 0.55	13	
Scyllo	0.12 ± 0.02	13	(n = 3)
Lac	1.89 ± 0.34	18	
NAA	8.38 ± 0.50	6	
NAAG	0.32 ± 0.12	38	(n = 3)
PE	1.98 ± 0.20	10	
Tau	4.25 ± 0.59	14	

Note. The concentrations were not corrected for T_1- and T_2-related signal decay. Metabolite concentrations were determined relative to [Cr + PCr] = (7.78 ± 0.58) μmol/g ww (CV = 7%) and were excluded from the total pool of measurements (n = 31) when the Cramér–Rao lower bounds of the LCModel analysis exceeded 35%. FWHM = 0.031 ± 0.004 ppm, S/N = 28 ± 5 (mean ± SD).

[a] All rats with glucose infusion were excluded from the analysis.

DISCUSSION

This study shows that the detailed features of short-echo-time *in vivo* spectra can be explained as a superposition of solution model spectra *plus* a background consisting of fast relaxing resonances (Figs. 5 and 6). The residual spline baseline was nearly negligible and thus, based on neurochemical extract data, no assumptions about major unknown metabolite contributions were needed to explain the *in vivo* data. Remarkable is the capability of LCModel to account for distorted baselines (*43*) or lineshapes, which may be caused by, e.g., eddy currents or a not fully suppressed water resonance. Despite excellent shimming, outer volume suppression, and a well-defined localization that minimized experimental artifacts, the fitted LCModel spline baseline of our *in vivo* ^{1}H spectra (Fig. 1) was very structured and nonnegligible. This observation supports previous findings that macromolecules with short T_1 and T_2 are detected *in vivo* by ^{1}H spectroscopy (*14*, *44–46*).

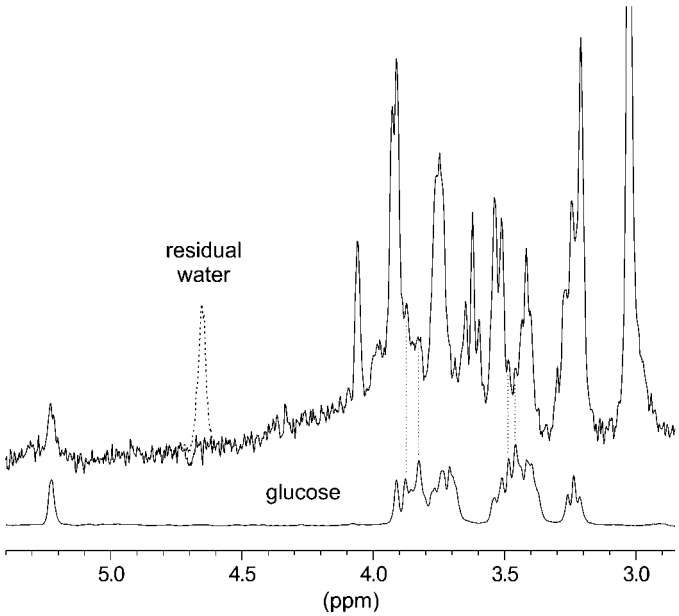

FIG. 9. ^{1}H NMR spectrum of the rat brain *in vivo* during glucose infusion (4 mg/min) and fitted glucose model spectrum. LCModel analysis was performed in the spectral region up to 5.4 ppm including the α-Glc H1 resonance at 5.226 ppm (TE = 20 ms, TM = 20 ms, TR = 4 s). The brain glucose concentration was determined to be 5.2 μmol/g ww (CR = 4%). Note the excellent agreement of the fine structure of the fitted glucose model spectrum with the *in vivo* data (dotted lines). The residual water signal at 4.65 ppm (dashed curve) was removed in the time domain prior to the analysis with LCModel. Only FT and zero-order phase correction was applied to the *in vivo* data (no weighting function).

Baseline in Short-Echo-Time Spectra

The metabolite T_2 values were between 100 and 150 ms (Table 2), consistent with previous *in vivo* reports at 7–9.4 T (*47–49*). Longer T_2 (180–260 ms) was reported at 4.7 T (*50*). Since the macromolecule T_2^{MM} was several times shorter at 9.4 T, i.e., approximately 26 ms, their contribution to the spectrum could be minimized by using longer echo times, e.g., TE = 100 ms (Fig. 2), at the expense of increased sensitivity to T_2 changes and reduced information content. At short echo times the macromolecule background is present in the entire ^{1}H chemical shift range from 4.3 to 0.8 ppm, i.e., approximately 10% of the MM signals are still left at TE = 60 ms. From the resolved macromolecule intensities of the M1–M4 peaks, the overall macromolecule contributions to the ^{1}H spectrum can be assessed, provided that outer volume contaminations have been minimized. In our experimental setup, excellent localization with outer volume suppression was achieved using methods reported elsewhere (*27*).

The metabolite T_1 values of the CH_3 groups (approximately 1.4 s, Table 2) measured at 9.4 T were similar for Cho, Cr, and NAA and lie in the range of those (1.4–1.9 s) reported at 7 T (*48*) and 4.7 T (*50*). However, the macromolecule $T_1^{MM} \sim 300$ ms was considerably shorter, which was exploited to determine the macromolecule background at 2-ms echo time, consistent with previous studies (*45*, *46*). As shown in Fig. 3, our results and peak positions of the macromolecules, observed between 4.3 and 0.5 ppm, agreed very well with previous studies of rat and human brain tissue separating low- and high-molecular-weight cytosolic fractions (*14*). In addition, the diffusion coefficient of the macromolecules was found to be 50 times lower than that of freely diffusing water (*51*), which corresponds to their large molecular weight.

The additional spline baseline with wide knot spacing of 0.25 ppm can be interpreted as a weight of the MM model spectrum in different spectral regions, which may be attributed to small T_1 differences within the MM resonances. This can, for instance, be seen in Fig. 5, where the residual spline baseline is higher at ~3.7 ppm and lower at ~2.5 ppm. Including an experimentally measured MM spectrum in the LCModel analysis reproduced all major *in vivo* spectral features, with the exception of ASP at 2.79 ppm, which may have been underestimated due to a strong peak at 2.68 ppm in the MM spectrum, which might be a residual of the NAA βCH_2 resonance with shorter T_1.

Principally, a systematic error in the MM baseline might be introduced by an incomplete nulling of the metabolite signals at a given t_{IR}^{null}. Incomplete nulling can be caused by differences in the metabolite T_1 at TE = 2 ms from T_1 of Cr and NAA at

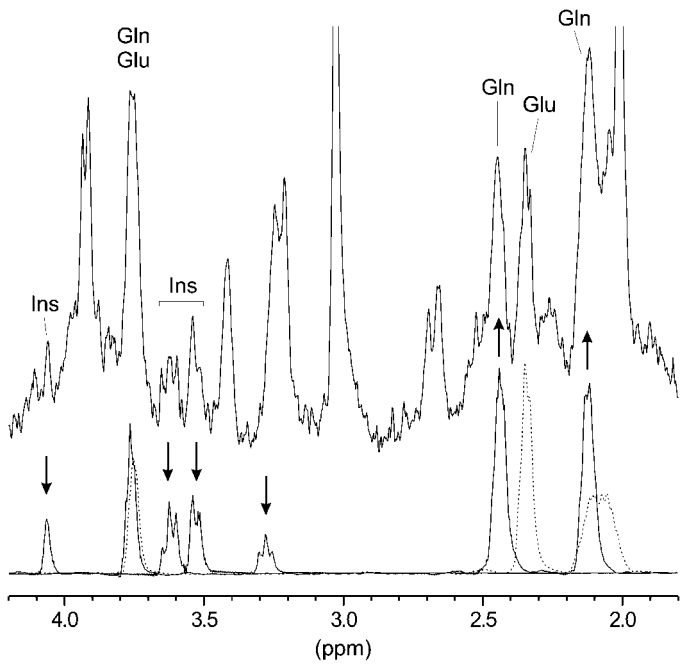

FIG. 10. Short-echo-time ^{1}H NMR spectrum of a rat with threefold elevated glutamine (hepatic encephalopathy) and decreased *myo*-inositol (TE = 2 ms, TM = 20 ms, TR = 4 s). Solution model spectra of *myo*-inositol, glutamine (solid curves), and glutamate (dotted curve) are shown as fitted by LCModel. Note the full separation of glutamine and glutamate resonances in positions γCH_2 and βCH_2. Only FT and zero-order phase correction was applied to the *in vivo* data (no weighting function).

TE = 100 ms (Fig. 2). The nulling times of Glu, Gln, Ins, Tau, or GABA were not found to be different in a series of short-echo-time spectra with inversion times from 0.1 to 3 s. Residual coupling patterns were not observed using resolution enhancement of the spectrum at $t_{IR}^{null} = 0.95$ s (data not shown). Except for the shorter T_1 for the methylene Cr + PCr at 3.9 ppm, there was no experimental evidence that relaxation times vary substantially among the metabolites. This is supported by the observation that T_1 for Cr was found to be comparable to that of GABA at 4 T in the human brain (*46*), to that of Glc in the human brain (*52*), and to T_1 of Glu in the rat brain at 7 T (*48*). The spline baseline overall represented the macromolecule signals well, which further supports the notion that residual narrow metabolite signals are minor in metabolite-nulled spectra.

Quantification

Comparison of the metabolite concentrations obtained at 9.4 T from the rat brain *in vivo* with neurochemical literature mostly from the rat brain (Table 3) showed very good overall agreement. However, a direct comparison to the neurochemical concentrations may be subject to different experimental conditions such as different animals, regional variability of the metabolite concentrations, or methodological uncertainties of the extraction process as pointed out in, e.g., Ref. (*13*). The concentrations of Ala, Cho, Cr, PCr, NAA, PE, and Tau were highly consistent with the neurochemical literature data, whereby our *in vivo* quantification was based on the assumption of a constant tissue water content of 83% (internal water reference). The concentrations of Asp, GABA, Gln, Glu, and GSH were comparable as well, but tended to provide lower values than the literature data. Although in the high-quality spectra (Figs. 6 and 7) the concentrations of Gln relative to Cr + PCr were not changed between TE = 2 and 20 ms, it was observed that in the medium quality spectra with TE = 20 ms (Table 5) the Gln concentration was decreased and had a relatively large interassay standard deviation. This points to the fact that, even at 9.4 T, quantification of Gln was difficult without excellent shimming. The concentrations of Lac tended to be higher than in the literature (about 1.5–2.5 μmol/g ww) and revealed some variability between animals. For Tau, the literature data show a considerable variation, because its concentration strongly depends on the area in the brain (*33*), which may be true for Gln, too.

The serine contribution was found to be insignificant in the spectra compared to PE. Evidence for the presence of a PE signal in ^{1}H NMR spectra was found in the literature: 2D ^{1}H *J*-resolved spectra of extract data (*13*) revealed a compound near 4.0 ppm (not assigned) with a homonuclear coupling of $J_{HH} \sim 5$ Hz and a small heteronuclear splitting (J_{PH}), which matches our solution spectrum of PE ($J_{HH} = 5.0$ Hz, $J_{PH} = 7.2$ Hz). A cross peak of PE with coordinates (4.0, 3.2 ppm) was detected in 2D ^{1}H COSY experiments in rat brain tumors *in vivo* (*53*). *In vivo* ^{31}P NMR studies as well as neurochemical data showed a considerable contribution of PE in the brain on the order of 2 mM (*33, 54, 55*). Further experiments are needed to determine relative contributions of glycerophosphorylethanolamine to the ^{1}H NMR resonance at 3.98 ppm *in vivo* (*56, 57*).

Quantification of glycine, another important neurotransmitter, which is present in significant concentrations in the brain, was difficult, because the singlet resonance at 3.55 ppm overlapped with the [1,3]CH inositol resonance. Using long echo times or two-dimensional methods, e.g., CT-PRESS for effective homonuclear decoupling, may be needed to distinguish the glycine signal *in vivo* (*58, 59*).

The influences of T_2 on quantification are difficult to unravel and depend on the experimental parameters used. In the model spectra, T_2 was so long (>600 ms) that its effect on the signals at short echo time was negligible. Cr and NAA signals were attenuated *in vitro* by approximately 4 and 2% at TE = 20 ms. Considering that T_2 was shorter *in vivo* (~100 ms) and showed inter- and intrametabolite variations, a correction factor for each metabolite concentration was, therefore, not trivial to determine even at short echo times of TE = 20 ms. Measurements of the metabolite signals and the water reference at TE = 2 ms minimized such effects.

An excellent match between the *in vitro* spectral patterns with the *in vivo* data was achieved by carefully adjusting pH of the metabolite model solutions and by controlling the temperature. For example, the Cr methylene resonance shifted by approximately 0.1 Hz/°C, which affected the analysis at 9.4 T, since the separation of the Cr and PCr methylene signals was only 8 Hz *in vivo*. The chemical shifts of the *myo*-inositol multiplets changed by less than 0.3 Hz/°C, which nevertheless influenced multiplet intensities due to higher order spin effects.

The total creatine, NAA, and the sum of Gln + Glu concentrations measured at TE = 20 ms (Table 3 to 5) agree well with a previous study that used the LCModel approach in the rat brain *in vivo* at 2.35 T (*41*). In our study, the Tau concentration was higher and Cho lower, which can be explained by the reduced resolution between Tau–Cho and a concomitant increase in the Cramér–Rao lower bounds at lower fields. Coefficients of variation in the current study were up to *eight* times smaller when correcting for differences in voxel size. Such increases in sensitivity can only partially be explained by the increase in static field, since the improved resolution significantly contributes to the overall sensitivity. This is evident when considering, for instance, that total creatine exhibits a 4-fold increase in sensitivity, which is half that observed for *myo*-inositol. The importance of the spectral resolution in improving sensitivity can be further appreciated when considering that at 9.4 T PCr is now a separately quantifiable metabolite, which could be interpreted either as an at least 100-fold gain in SNR for PCr or simply that the number of identified metabolites was dramatically increased. Therefore, many metabolites can be more reliably assessed at high magnetic fields

due to their increasingly distinguishable representation in the spectra, e.g., PCr and Cr, Gln and Glu, Tau and Cho, PE, GABA, GSH, and Ala.

A recent study using time domain fitting in the rat brain *in vivo* at 4.7 T (TE = 16 ms) included the major metabolites NAA, Glu, Gln, Cr, Cho, Glc, and Ins (*19*), which agreed with our measurements within their large interassay variation. A much higher Cho concentration of 0.2–0.3 times of [Cr + PCr] was reported, which can be explained by the absence of taurine in their analysis. Quantification of glutamine at 4.7 T in the rat brain yielded a CR of 100% suggesting a low reliability. The ability to detect the changes of glutamine in the human brain at 4 T much more accurately (*26*) further illustrated the advantages of excellent shimming. At 9.4 T, the glutamine and glutamate γCH_2 resonances were fully separated and the βCH_2 resonances show a distinct pattern that can be separated using deconvolution algorithms such as LCModel.

In addition to the well-resolved glucose peak at 5.226 ppm, also detected and resolved at 4 T (*52, 60*), a distinct spectral representation of glucose was observed at 3.9 to 3.4 ppm in 9.4-T spectra from the rat brain. However, even under hyperglycemic conditions, the peak at 3.4 ppm is a triplet and thus closely resembles that of the taurine model spectrum as shown in Fig. 9, further supporting the observation that the glucose signal is a minor constituent at this chemical shift in the brain (*15, 61*). Detection of resolved glucose resonances may be critical in achieving the needed accuracy for glucose measurements by ^{1}H NMR.

Extensions to other deconvolution methods are possible, although it remains to be demonstrated that other quantification methods, e.g., time domain fitting with prior knowledge (*21, 62*), principal component (*22*) or wavelet analysis (*23*), are able to handle such large sets of model spectra, containing multiple resonances, and that they are equally robust. It also remains to be shown whether the accuracy and efficiency of quantification of metabolites with low concentrations can be improved using alternate methods, which focus on the detection of selected metabolites, e.g., spectral editing of GABA (*46*) or using 2D fitting of multiple echo times (*21*).

CONCLUSIONS

Ultrashort echo times combined with high sensitivity achieved at 9.4 T and excellent shimming maximize the spectral information in localized ^{1}H NMR spectra of the rat brain *in vivo* with minimal T_2 relaxation or *J*-modulation effects. We conclude that the *in vivo* spectra can be fully described by a superposition of 18 metabolite solution spectra and a macromolecule background with short T_1 relaxation times. This includes the simultaneous quantification of phosphocreatine, phosphorylethanolamine, GABA, glutathione, alanine, aspartate, resting lactate, and completely resolved glutamine in ^{1}H NMR spectra without any editing. Using high-field NMR with excellent shimming may lead to a noninvasive assessment of a significantly expanded neurochemical profile *in vivo* and time-resolved functional NMR spectroscopy (*63*) for the study of animal models of disease, e.g., hypoxia, stroke, or hepatic encephalopathy. Considering the significant resolution improvements with high static magnetic field shown in the human brain (*26, 64, 65*), human studies should also benefit from increased magnetic fields.

ACKNOWLEDGMENTS

The authors thank Kamil Ugurbil, Michael Garwood, Keiko Kanamori, and Dieter Leibfritz for helpful discussions and In-Young Choi for the construction of the RF probe. The HLSVD routine as part of the MRUI software package was obtained from the MRUI PROJECT. This work was supported by National Institutes of Health Grants R01 CA64338 and P41 RR08079 and by the W. M. Keck Foundation.

REFERENCES

1. F. A. Howe, R. J. Maxwell, D. E. Saunders, M. M. Brown, and J. R. Griffiths, Proton spectroscopy in vivo, *Magn. Reson. Q.* **9,** 31–59 (1993).
2. B. D. Ross and T. Michaelis, Clinical applications of magnetic resonance spectroscopy, *Magn. Reson. Q.* **10,** 191–247 (1994).
3. M. W. Weiner, H. P. Hetherington, B. Hubesch, G. Karczmar, B. Massie, A. A. Maudsley, D. J. Meyerhoff, D. Sappey-Marinier, S. Schaefer, and D. B. Twieg, Clinical magnetic resonance spectroscopy of brain, heart, liver, kidney, and cancer. A quantitative approach. [Review], *NMR Biomed.* **2,** 290–297 (1989).
4. D. G. Gadian, T. E. Bates, S. R. Williams, J. D. Bell, S. J. Austin, and A. Connelly, Approaches to editing, assignment and interpretation of proton spectra, *NMR Biomed.* **4,** 85–89 (1991).
5. S. R. Williams, Cerebral amino acids studied by nuclear magnetic resonance spectroscopy in vivo, *Prog. NMR Spectrosc.* **34,** 301–326 (1999).
6. J. A. Stanley, D. J. Drost, P. C. Williamson, and R. T. Thompson, The use of a priori knowledge to quantify short echo in vivo 1H MR spectra, *Magn. Reson. Med.* **34,** 17–24 (1995).
7. J. H. Hwang, G. D. Graham, K. L. Behar, J. R. Alger, J. W. Prichard, and D. L. Rothman, Short echo time proton magnetic resonance spectroscopic imaging of macromolecule and metabolite signal intensities in the human brain, *Magn. Reson. Med.* **35,** 633–639 (1996).
8. D. E. Saunders, F. A. Howe, A. van den Boogaart, J. R. Griffiths, and M. M. Brown, Discrimination of metabolite from lipid and macromolecule resonances in cerebral infarction in humans using short echo proton spectroscopy, *J. Magn. Reson. Imaging* **7,** 1116–1121 (1997).
9. P. J. Pouwels and J. Frahm, Differential distribution of NAA and NAAG in human brain as determined by quantitative localized proton MRS, *NMR Biomed.* **10,** 73–78 (1997).
10. W. Willker, J. Engelmann, A. Brand, and D. Leibfritz, Metabolite identification in cell extracts and culture media by proton-detected 2D-H,C-NMR spectroscopy, *J. Magn. Reson. Anal.* **2,** 21–32 (1996).
11. J. Peeling and G. Sutherland, ^{1}H magnetic resonance spectroscopy of extracts of human epileptic neocortex and hippocampus, *Neurology* **43,** 589–594 (1993).
12. S. Cerdan, R. Parrilla, J. Santoro, and M. Rico, ^{1}H NMR detection of cerebral myo-inositol, *FEBS Lett.* **187,** 167–172 (1985).

13. O. A. Petroff, T. Ogino, and J. R. Alger, High-resolution proton magnetic resonance spectroscopy of rabbit brain: Regional metabolite levels and postmortem changes, *J. Neurochem.* **51,** 163–171 (1988).
14. K. L. Behar and T. Ogino, Characterization of macromolecule resonances in the ^{1}H NMR spectrum of rat brain, *Magn. Reson. Med.* **30,** 38–44 (1993).
15. W. Dreher and D. Leibfritz, On the use of two-dimensional-J NMR measurements for in vivo proton MRS: Measurement of homonuclear decoupled spectra without the need for short echo times, *Magn. Reson. Med.* **34,** 331–337 (1995).
16. I. M. Brereton, G. J. Galloway, S. E. Rose, and D. M. Doddrell, Localized two-dimensional shift correlated spectroscopy in humans at 2 Tesla, *Magn. Reson. Med.* **32,** 251–257 (1994).
17. E. R. Seaquist and R. Gruetter, Identification of a high concentration of scyllo-inositol in the brain of a healthy human subject using ^{1}H- and ^{13}C-NMR, *Magn. Reson. Med.* **39,** 313–316 (1998).
18. R. de Beer and D. van Ormondt, Analysis of NMR data using time domain fitting procedures, *NMR Basic Princ. Prog.* **26,** 201–248 (1992).
19. S. Mierisova, A. van den Boogaart, I. Tkac, P. Van Hecke, L. Vanhamme, and T. Liptaj, New approach for quantitation of short echo time in vivo 1H MR spectra of brain using AMARES, *NMR Biomed.* **11,** 32–39 (1998).
20. S. W. Provencher, Estimation of metabolite concentrations from localized in vivo proton NMR spectra, *Magn. Reson. Med.* **30,** 672–679 (1993).
21. J. Slotboom, C. Boesch, and R. Kreis, Versatile frequency domain fitting using time domain models and prior knowledge, *Magn. Reson. Med.* **39,** 899–911 (1998).
22. R. Stoyanova, A. C. Kuesel, and T. R. Brown, Application of principal-component analysis for NMR spectral quantitation, *J. Magn. Reson. A* **115,** 265–269 (1995).
23. B. J. Soher, K. Young, V. Govindaraju, and A. A. Maudsley, Automated spectral analysis III: Application to in vivo proton MR spectroscopy and spectroscopic imaging, *Magn. Reson. Med.* **40,** 822–831 (1998).
24. G. J. Metzger, M. Patel, and X. Hu, Application of genetic algorithms to spectral quantification, *J. Magn. Reson. B* **110,** 316–320 (1996).
25. O. M. Weber, C. O. Duc, D. Meier, and P. Boesiger, Heuristic optimization algorithms applied to the quantification of spectroscopic data, *Magn. Reson. Med.* **39,** 723–730 (1998).
26. R. Gruetter, S. A. Weisdorf, V. Rajanayagan, M. Terpstra, H. Merkle, C. L. Truwit, M. Garwood, S. L. Nyberg, and K. Ugurbil, Resolution improvements in in vivo ^{1}H NMR spectra with increased magnetic field strength, *J Magn. Reson.* **135,** 260–264 (1998).
27. I. Tkac, Z. Starcuk, I. Y. Choi, and R. Gruetter, In vivo ^{1}H NMR spectroscopy of rat brain at 1 ms echo time, *Magn. Reson. Med.* **41,** 649–656 (1999).
28. M. Terpstra, P. M. Andersen, and R. Gruetter, Localized eddy current compensation using quantitative field mapping, *J. Magn. Reson.* **131,** 139–143 (1998).
29. G. Adriany and R. Gruetter, A half-volume coil for efficient proton decoupling in humans at 4 Tesla, *J. Magn. Reson.* **125,** 178–184 (1997).
30. A. Tannus and M. Garwood, Improved performance of frequency-swept pulses using offset-independent adiabaticity, *J. Magn. Reson. A* **120,** 133–137 (1996).
31. R. Gruetter, Automatic, localized in vivo adjustment of all first- and second-order shim coils, *Magn. Reson. Med.* **29,** 804–811 (1993).
32. W. W. F. Pijnappel, A. van den Boogaart, R. de Beer, and D. van Ormondt, SVD-based quantification of magnetic resonance signals, *J. Magn. Reson.* **97,** 122–134 (1992).
33. H. McIlwain and H. S. Bachelard, "Biochemistry and the Central Nervous System," 5th ed., Churchill Livingstone, Edinburgh (1985).
34. T. L. Perry, Cerebral amino acid pools, *in* "Handbook of Neurochemistry" (A. Lajtha, Ed.), 2nd ed., Vol. 1, pp. 151–180, Plenum Press, New York (1982).
35. D. D. Clarke, A. L. Lajtha, and H. S. Maher, Intermediary metabolism, *in* "Basic Neurochemistry" (G. J. Siegel, Ed.), pp. 541–564, Raven, New York (1989).
36. R. L. Veech, R. L. Harris, D. Veloso, and E. H. Veech, Freeze-blowing: A new technique for the study of brain in vivo, *J. Neurochem.* **20,** 183–188 (1973).
37. A. M. Mans, M. R. DeJoseph, and R. A. Hawkins, Metabolic abnormalities and grade of encephalopathy in acute hepatic failure, *J. Neurochem.* **63,** 1829–1838 (1994).
38. D. Holowenko, J. Peeling, and G. Sutherland, 1H NMR properties of N-acetylaspartylglutamate in extracts of nervous tissue of the rat, *NMR Biomed.* **5,** 43–47 (1992).
39. R. K. Shaw and J. D. Heine, Effect of insulin on nitrogenous constituents of rat brain, *J. Neurochem.* **12,** 527–532 (1965).
40. L. Battistin and A. Lajtha, Regional distribution and movement of amino acids in the brain, *J. Neurol. Sci.* **10,** 313–322 (1970).
41. Y. Nagatomo, M. Wick, F. Prielmeier, and J. Frahm, Dynamic monitoring of cerebral metabolites during and after transient global ischemia in rats by quantitative proton NMR spectroscopy in vivo, *NMR Biomed.* **8,** 265–270 (1995).
42. B. D. Ross, E. R. Danielsen, and S. Bluml, Proton magnetic resonance spectroscopy: The new gold standard for diagnosis of clinical and subclinical hepatic encephalopathy?, *Dig. Dis.* **14**(Suppl. 1), 30–39 (1996).
43. S. W. Provencher, Automated quantitation of localized ^{1}H MR spectra *in vivo* at short echo times with baseline distortion, *Proc. ISMRM, 5th Sci. Meet., Vancouver.* 1411 (1997).
44. D. L. Rothman, K. L. Behar, J. W. Prichard, and O. A. Petroff, Homocarnosine and the measurement of neuronal pH in patients with epilepsy, *Magn. Reson. Med.* **38,** 924–929 (1997).
45. K. L. Behar, D. L. Rothman, D. D. Spencer, and O. A. Petroff, Analysis of macromolecule resonances in ^{1}H NMR spectra of human brain, *Magn. Reson. Med.* **32,** 294–302 (1994).
46. M. Mescher, H. Merkle, J. Kirsch, M. Garwood, and R. Gruetter, Simultaneous in vivo spectral editing and water suppression, *NMR Biomed.* **11,** 266–272 (1998).
47. S. R. Williams, E. Proctor, K. Allen, D. G. Gadian, and H. A. Crockard, Quantitative estimation of lactate in the brain by ^{1}H NMR, *Magn. Reson. Med.* **7,** 425–431 (1988).
48. W. D. Rooney, T. Ebisu, A. Mancuso, S. Graham, M. W. Weiner, and A. A. Maudsley, Metabolite ^{1}H relaxation in normal and hyponatremic brain, *Magn. Reson. Med.* **35,** 688–696 (1996).
49. J. Kuhmonen, J. Sivenius, P. J. S. Riekkinen, and R. A. Kauppinen, Decrease in brain choline-containing compounds following a short period of global ischemia in gerbils as detected by ^{1}H NMR spectroscopy in vivo, *NMR Biomed.* **7,** 231–236 (1994).
50. A. van der Toorn, R. M. Dijkhuizen, C. A. Tulleken, and K. Nicolay, T_1 and T_2 relaxation times of the major ^{1}H-containing metabolites in rat brain after focal ischemia, *NMR Biomed.* **8,** 245–252 (1995).

51. J. Pfeuffer, I. Tkac, and R. Gruetter, Diffusion-weighted *in vivo* ^{1}H NMR spectroscopy of brain glucose and metabolites, *Magma* **6**(Suppl. 1), 9 (1998).

52. R. Gruetter, K. Ugurbil, and E. R. Seaquist, Steady-state cerebral glucose concentrations and transport in the human brain, *J. Neurochem.* **70,** 397–408 (1998).

53. A. Ziegler, M. Izquierdo, C. Remy, and M. Decorps, Optimization of homonuclear two-dimensional correlation methods for *in vivo* and *ex vivo* NMR, *J. Magn. Reson. B* **107,** 10–18 (1995).

54. R. J. Corbett, A. R. Laptook, A. Hassan, and R. L. Nunnally, Quantitation of acidosis in neonatal brain tissue using the ^{31}P NMR resonance peak of phosphoethanolamine, *Magn. Reson. Med.* **6,** 99–106 (1988).

55. R. Burri, F. Lazeyras, W. P. Aue, P. Straehl, P. Bigler, U. Althaus, and N. Herschkowitz, Correlation between ^{31}P NMR phosphomonoester and biochemically determined phosphorylethanolamine and phosphatidylethanolamine during development of the rat brain, *Dev. Neurosci.* **10,** 213–221 (1988).

56. M. Ala-Korpela, P. Posio, S. Mattila, A. Korhonen, and S. R. Williams, Absolute quantification of phospholipid metabolites in brain-tissue extracts by ^{1}H NMR spectroscopy, *J. Magn. Reson. B* **113,** 184–189 (1996).

57. S. Bluml, E. Zuckerman, J. Tan, and B. D. Ross, Proton-decoupled ^{31}P magnetic resonance spectroscopy reveals osmotic and metabolic disturbances in human hepatic encephalopathy, *J. Neurochem.* **71,** 1564–1576 (1998).

58. R. E. Hurd, D. Gurr, and N. Sailasuta, Proton spectroscopy without water suppression: The oversampled J- resolved experiment, *Magn. Reson. Med.* **40,** 343–347 (1998).

59. W. Dreher and D. Leibfritz, Detection of homonuclear decoupled in vivo proton NMR spectra using constant time chemical shift encoding: CT-PRESS, *Magn. Reson. Imaging* **17,** 141–150 (1999).

60. R. Gruetter, M. Garwood, K. Ugurbil, and E. R. Seaquist, Observation of resolved glucose signals in ^{1}H NMR spectra of the human brain at 4 Tesla, *Magn. Reson. Med.* **36,** 1–6 (1996).

61. R. Gruetter, E. J. Novotny, S. D. Boulware, D. L. Rothman, and R. G. Shulman, ^{1}H NMR studies of glucose transport in the human brain, *J. Cereb. Blood Flow Metab.* **16,** 427–438 (1996).

62. R. de Beer, A. van den Boogaart, D. van Ormondt, W. W. Pijnappel, J. A. den Hollander, A. J. Marien, and P. R. Luyten, Application of time-domain fitting in the quantification of in vivo ^{1}H spectroscopic imaging data sets, *NMR Biomed.* **5,** 171–178 (1992).

63. J. Pfeuffer, I. Tkac, I. Y. Choi, H. Merkle, K. Ugurbil, M. Garwood, and R. Gruetter, Localized in vivo ^{1}H NMR detection of neurotransmitter labeling in rat brain during infusion of [1-^{13}C] D-glucose, *Magn. Reson. Med.* **41,** 1077–1083 (1999).

64. S. Posse, C. A. Cuenod, R. Risinger, D. Le Bihan, and R. S. Balaban, Anomalous transverse relaxation in ^{1}H spectroscopy in human brain at 4 Tesla, *Magn. Reson. Med.* **33,** 246–252 (1995).

65. H. P. Hetherington, J. W. Pan, W. J. Chu, G. F. Mason, and B. R. Newcomer, Biological and clinical MRS at ultra-high field, *NMR Biomed.* **10,** 360–371 (1997).